

# **Lecture 6. Interstellar Dust: Chemical & Thermal Properties**

1. Spectral Features and Size
2. Grain Populations and Models
3. Thermal Properties
4. Small Grains and Large Molecules
5. Grain Evolution (as time permits)

## **References**

Tielens, Chs. 5 & 6

J. S. Mathis, ARAA 28, 37, 1990

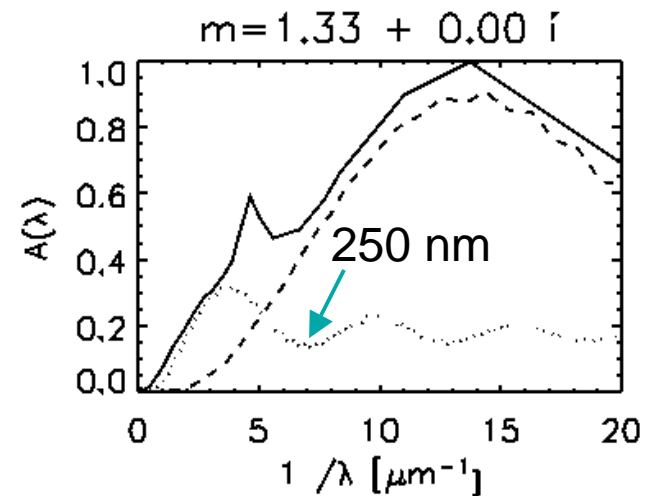
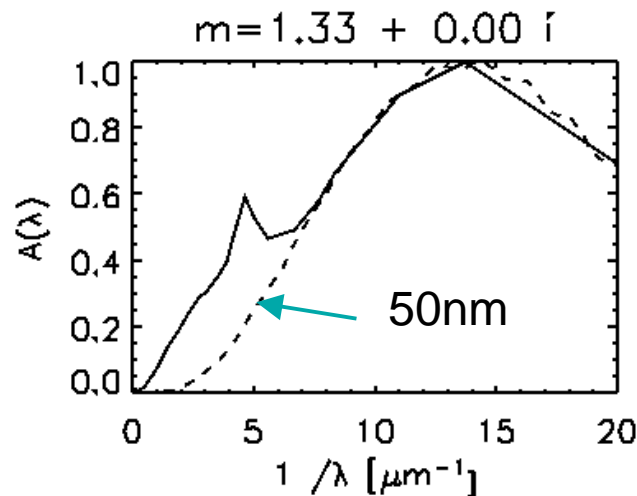
B. T. Draine, ARAA 41, 241, 1993

# 1. Spectral Features and Size

Recall the summary from the previous lecture:

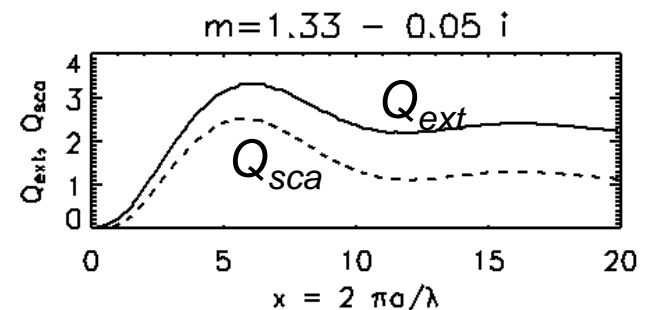
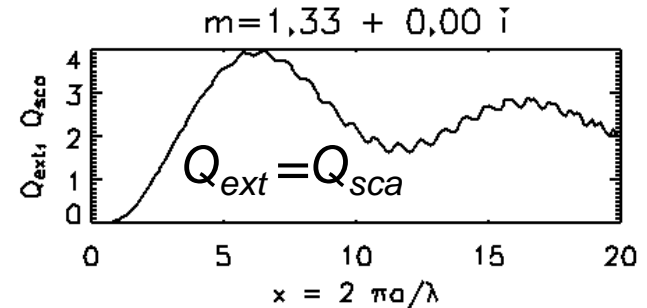
- The shape of the interstellar extinction curve contains information about the size and chemical composition of interstellar dust grains.
- The relatively smooth variation of the extinction with wavelength from 0.1 to 3  $\mu\text{m}$  indicates that a distribution of grain sizes are involved.
- The relatively large dust to gas ratio indicates that a substantial fraction of the heavy elements are bound up in dust
- The 220 nm bump and the 9.7 & 18  $\mu\text{m}$  features indicate the presence of C and Si, respectively,

# Shape of the Interstellar Extinction Curve

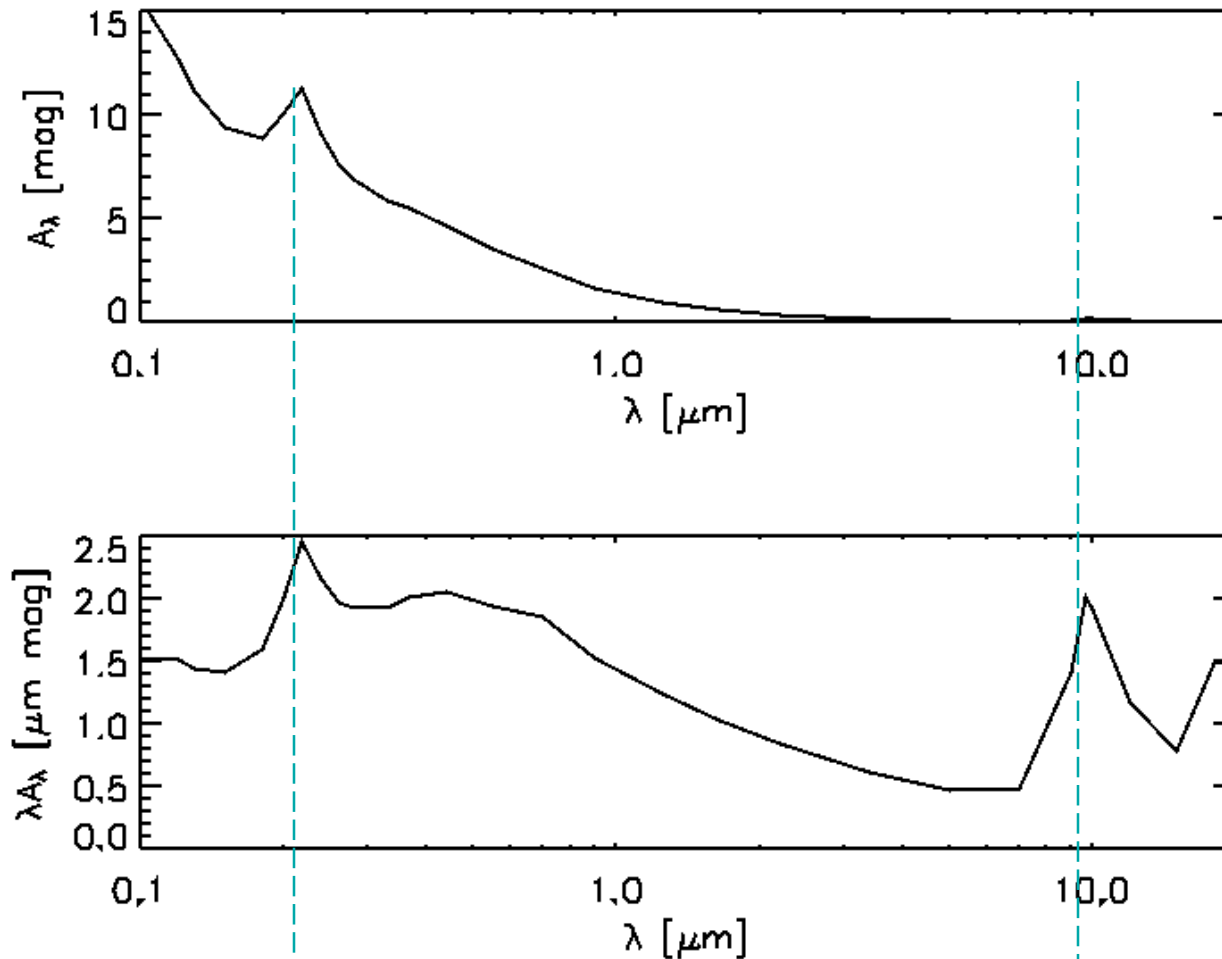


Toy water ice model with 50 & 250 nm grains, with small grains 90% by number, calculated by JRG and compared with Mathis' 1990 interstellar extinction curve (solid curve). Left: a single grain size can't explain the NIR/optical extinction. Right: Including larger grains helps.

The extinction curve does *not* look like a Mie  $Q_{\text{ext}}$  plot. The breadth suggests a distribution in sizes, with small grains more abundant than big ones



# Features in the Extinction Curve



2200 Å feature

10  $\mu\text{m}$  silicate feature

***The strongest dust spectral feature occurs at 220 nm***

# Role of Silicate Minerals

***Silicates have strong absorption resonances near 10  $\mu\text{m}$  due to the Si-O bond stretch*** (next slide).

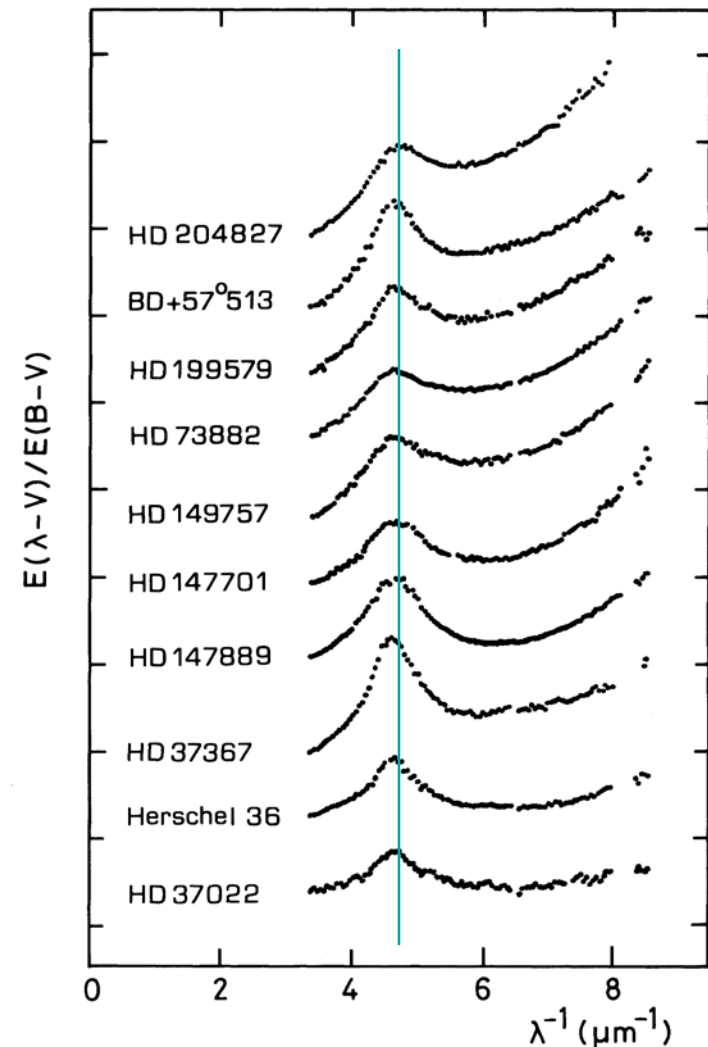
- It is virtually certain that the interstellar 9.7  $\mu\text{m}$  feature is produced by interstellar silicates (absorption as well as emission is observed).
- The 10  $\mu\text{m}$  emission feature is observed in outflows from cool O-rich stars
  - Their expanding atmospheres condense silicates
  - It is absent in the outflows from C-rich stars, where the O needed for silicates is all locked up in CO
  - The broad feature at 18  $\mu\text{m}$  can be identified with the O-Si-O bending mode in silicates

# Vibrational Modes of Silicate Minerals

	Species	Mode	Wavelength ( $\mu\text{m}$ )
enstatite	$\text{MgSiO}_3$	Si-O stretch	9.7
		O-Si-O bend	19.0
fosterite	$\text{Mg}_2\text{SiO}_4$	Si-O stretch	10.0
		O-Si-O bend	19.5
ferrosilite	$\text{FeSiO}_3$	Si-O stretch	9.5
		O-Si-O bend	20.0
fayalyte	$\text{Fe}_2\text{SiO}_4$	Si-O stretch	9.8
		O-Si-O bend	20.0
	$\text{SiC}$	SiC stretch	11.2

# The 220 nm Feature

- Ubiquitous in the Milky Way
  - $217.5 \pm 0.5$  nm (fixed wavelength)
  - width varies (10%) as does strength
- Graphite has a strong UV resonance due to  $\pi$ -orbital valence electrons
  - Why is the feature so uniform?
- 220 nm bump is weak in the SMC bar, presumably due to reduced C abundance
- Hydroxylated  $\text{Mg}_2\text{SiO}_4$  (fosterite) also has a 220 nm feature. (Steel & Duley 1986)



***The actual carrier of the 220 nm feature has not been identified.***

# 220 nm Feature in IDPs

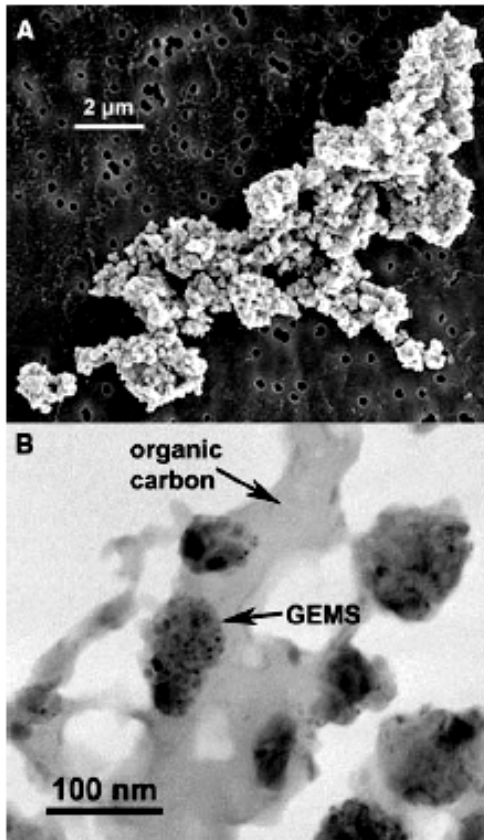


Fig. 2. (A) Secondary electron image of a typical chondritic IDP (RB12A). (B) A 200-keV brightfield transmission electron micrograph of organic carbon and GEMS within chondritic IDP L2009\*E2.

IDP = interplanetary dust particle

A. Interstellar 220 nm feature

B. Broad & narrow examples

C. lab: hydroxylated amorphous silicate

D. lab:  $\text{Mg}_3\text{Si}_4\text{O}_{10}[\text{OH}]_2$

E. IDP organic carbon

F. IDP silicates

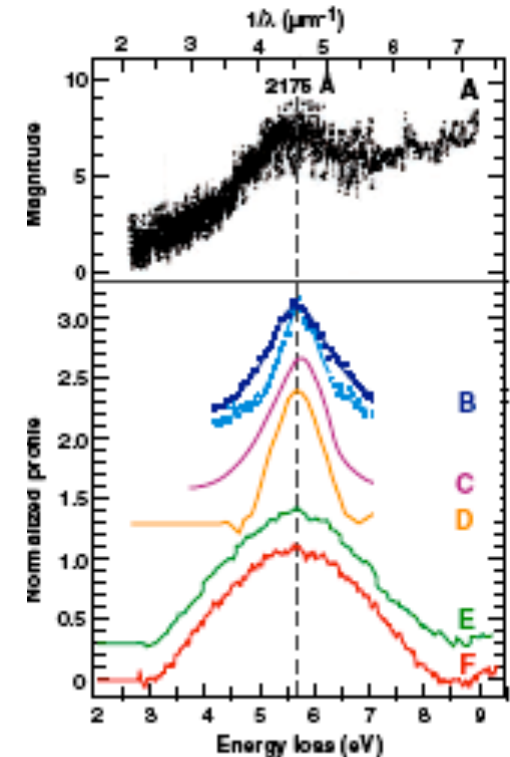


Fig. 1. Comparison of astronomical UV extinction features with laboratory UV and VEELS features. (A) The 2175 Å interstellar extinction feature from two stars ζ and ε Persei (5). (B) Broadest (ζ Oph) and narrowest (HD 93028) profiles from 45 stars (6). (C) Photoabsorption spectrum from partially recrystallized hydroxylated amorphous magnesium silicate (8). (D) VEELS spectrum from (electron) irradiation-damaged talc ( $\text{Mg}_3\text{Si}_4\text{O}_{10}[\text{OH}]_2$ ). (E) VEELS spectrum from (organic) carbon in IDP L2047 D23. (F) VEELS spectrum from GEMS in W7013 E17.

JP Bradley et al. Science, 307, 244, 2005: **Non-solar isotopic ratios indicate these IDPs are interstellar.**



## 2. Grain Populations

*There are at least three components associated with the optical/IR extinction, the 220 nm bump, and the FUV extinction rise.*

1. The rise in  $A_\lambda$  from the NIR/optical to the near UV requires  $a \sim 150$  nm, but if only 150 nm grains were present,  $A_\lambda$  for  $\lambda < 200$  nm would be approximately constant
2. The steep rise in FUV extinction down to 80 nm requires  $a \sim \lambda/2\pi \sim 15$  nm, otherwise  $Q_{\text{ext}}$  would be flat
3. The 220 nm bump implies a specific (unknown) carrier
  - symmetry and constancy of  $\lambda_0$  imply absorption in the small particle limit  $a \leq 10$  nm.
  - small graphite spheroids  $a \approx 3$  nm,  $b/a = 1.6$  might work, except for variation in central wavelength

# MRN Size Distribution

- Grain size distribution is likely to be continuous*  
(c.f. physical [coagulation] theory for small particle generation)
- Mathis, Rumpl & Nordseick (ApJ 217 425 1977)  
proposed power law distributions of graphite and  
silicate grains in approximately equal numbers

$$\frac{dn}{da} \propto A n_H a^{-3.5}, \quad a_{\min} < a < a_{\max}$$

$a_{\max} = 250$  nm, set by NIR and visible

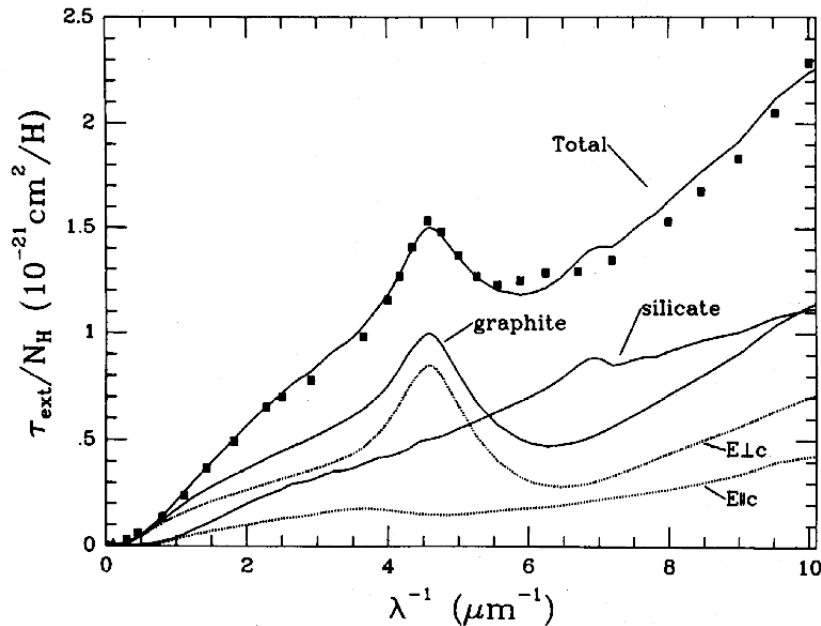
$a_{\min} = 5$  nm, set by FUV curve

- MRN power law has most of the mass in large particles &  
most of the area in small particles:

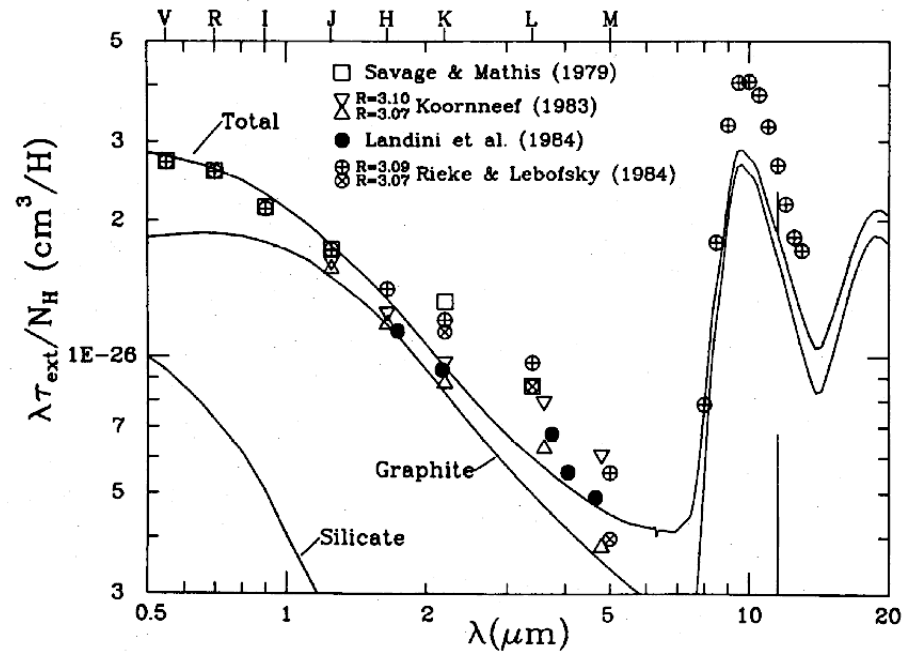
$$M \propto \int a^3 \frac{dn}{da} da \propto a_{\max}^{0.5} - a_{\min}^{0.5}$$

$$A \propto \int a^2 \frac{dn}{da} da \propto a_{\min}^{-0.5} - a_{\max}^{-0.5}$$

# Draine & Lee Model (ApJ 285 89 1984)



extinction expressed as cross section



comparison with other models

Two component MRN model:  $5\text{nm} < a < 250\text{nm}$

- Graphite: 60% of C
- “Astronomical silicate”: 90% of Si, 95 % Mg, 94% of Fe & 16% of O

# Draine & Lee: Silicates

10 & 20 micron  
silicate features

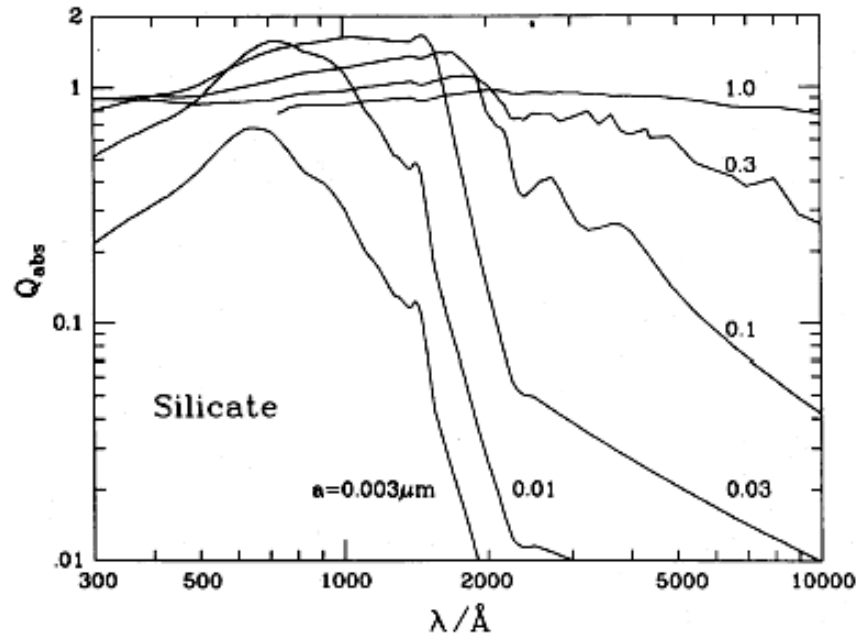


FIG. 5a

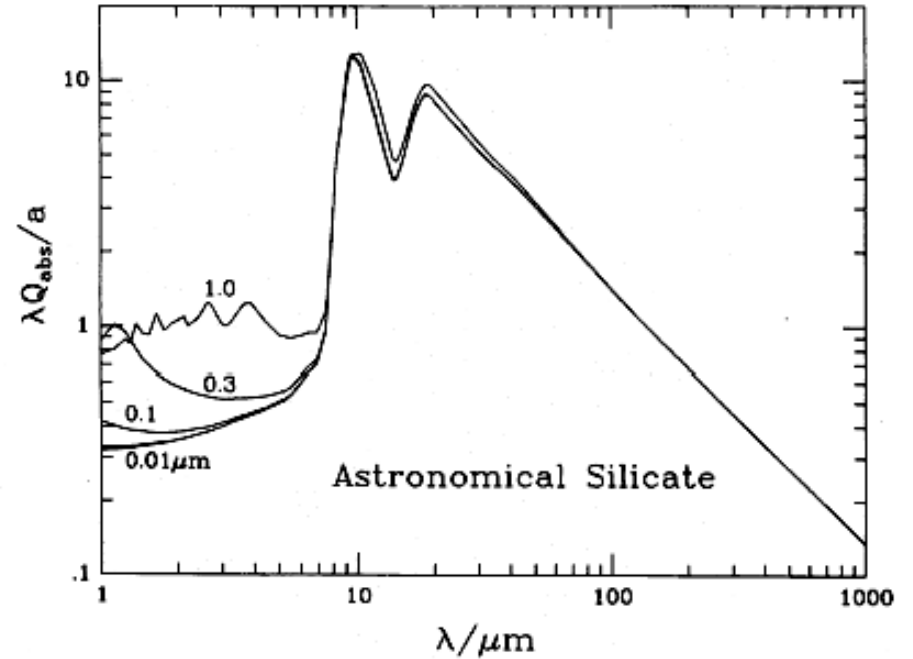


FIG. 5b

FIG. 5.—Absorption efficiencies  $Q_{\text{abs}}$  for spherical grains of “astronomical silicate” (curves are labeled by grain radius  $a$  in  $\mu\text{m}$ ). Note that for small grains ( $a \lesssim 0.1 \lambda$ ),  $Q_{\text{abs}} \propto a$ . (a)  $Q_{\text{abs}}$  for  $300 \text{\AA} < \lambda < 1 \mu\text{m}$ . (b)  $\lambda Q_{\text{abs}}/a$  for  $\lambda > 1 \mu\text{m}$ .

Silicate model for varying grain sizes.

Left: sub-micron wavelength

Right: NIR-FIR wavelengths

# Draine & Lee: Graphite

220nm feature  
for  $a < 300 \text{ \AA}$

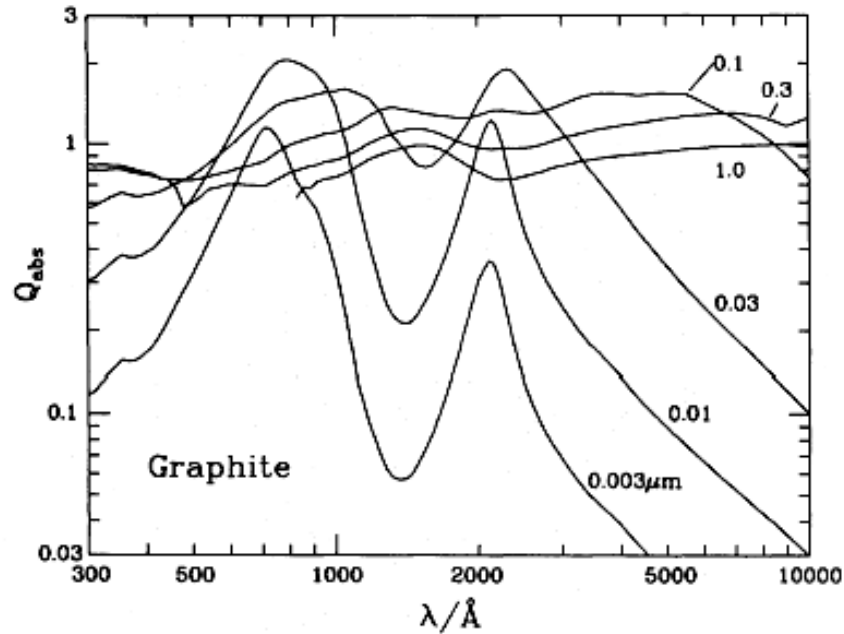


FIG. 4a

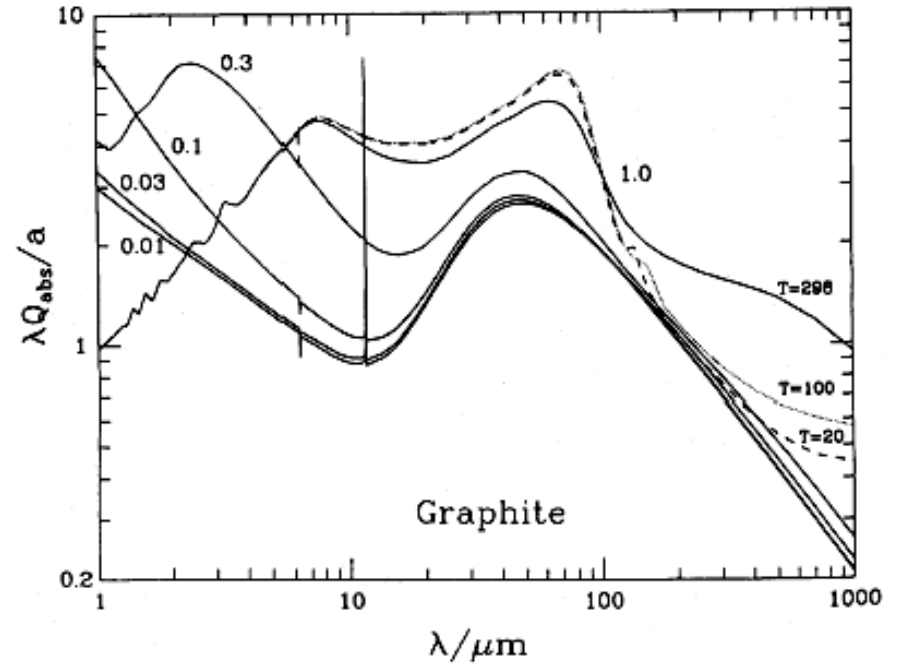


FIG. 4b

FIG. 4.—Absorption efficiencies  $Q_{\text{abs}}$  for spherical graphite grains (curves are labeled by grain radius  $a$  in  $\mu\text{m}$ ). (a)  $Q_{\text{abs}}$  for  $300 \text{ \AA} < \lambda < 1 \mu\text{m}$ . For small grains ( $a \lesssim 0.1 \lambda$ ),  $Q_{\text{abs}} \propto a$ . (b)  $\lambda Q_{\text{abs}}/a$  for  $\lambda > 1 \mu\text{m}$ . For  $a = 1 \mu\text{m}$ ,  $Q_{\text{abs}}$  has been computed at three different temperatures:  $T = 298 \text{ K}$ ,  $T = 100 \text{ K}$ , and  $T = 20 \text{ K}$ , labeled accordingly. For  $a \lesssim 0.3 \mu\text{m}$  the absorption cross sections are essentially independent of the grain temperature. In the limit  $a \rightarrow 0$ ,  $Q_{\text{abs}}/a$  is independent of  $a$ .

Graphite model for varying grain sizes.

Left: sub-micron wavelengths

Right: NIR-FIR wavelengths

# Weingartner & Draine Model (ApJ 598 246 2001)

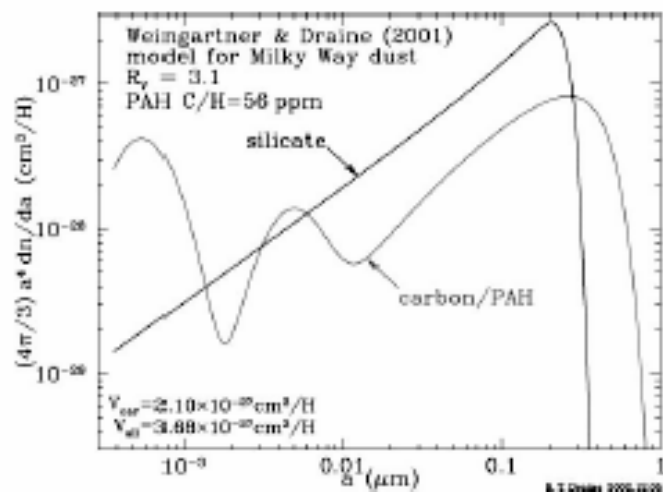


Figure 8 Size distributions for carbonaceous-silicate grain model of Weingartner & Draine (2001a) for Milky Way dust with  $R_V = 3.1$ , but with abundances decreased by a factor 0.93 (see text).

Above:  $a^4$  times the size distribution

Top right: submicron cross sections  
Bottom right: NIR-FIR cross sections

See Draine ARAA 41 241 2003  
for observational applications

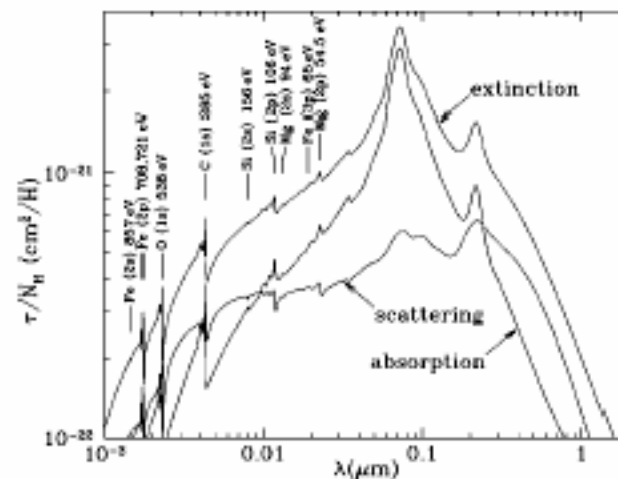


Figure 9 Extinction and scattering calculated for Weingartner & Draine (2001a) model for  $R_V = 3.1$  Milky Way dust, but with abundances reduced by factor 0.93 (see text).

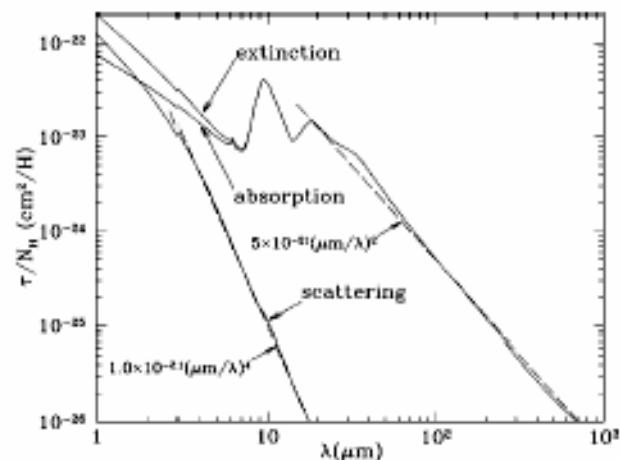
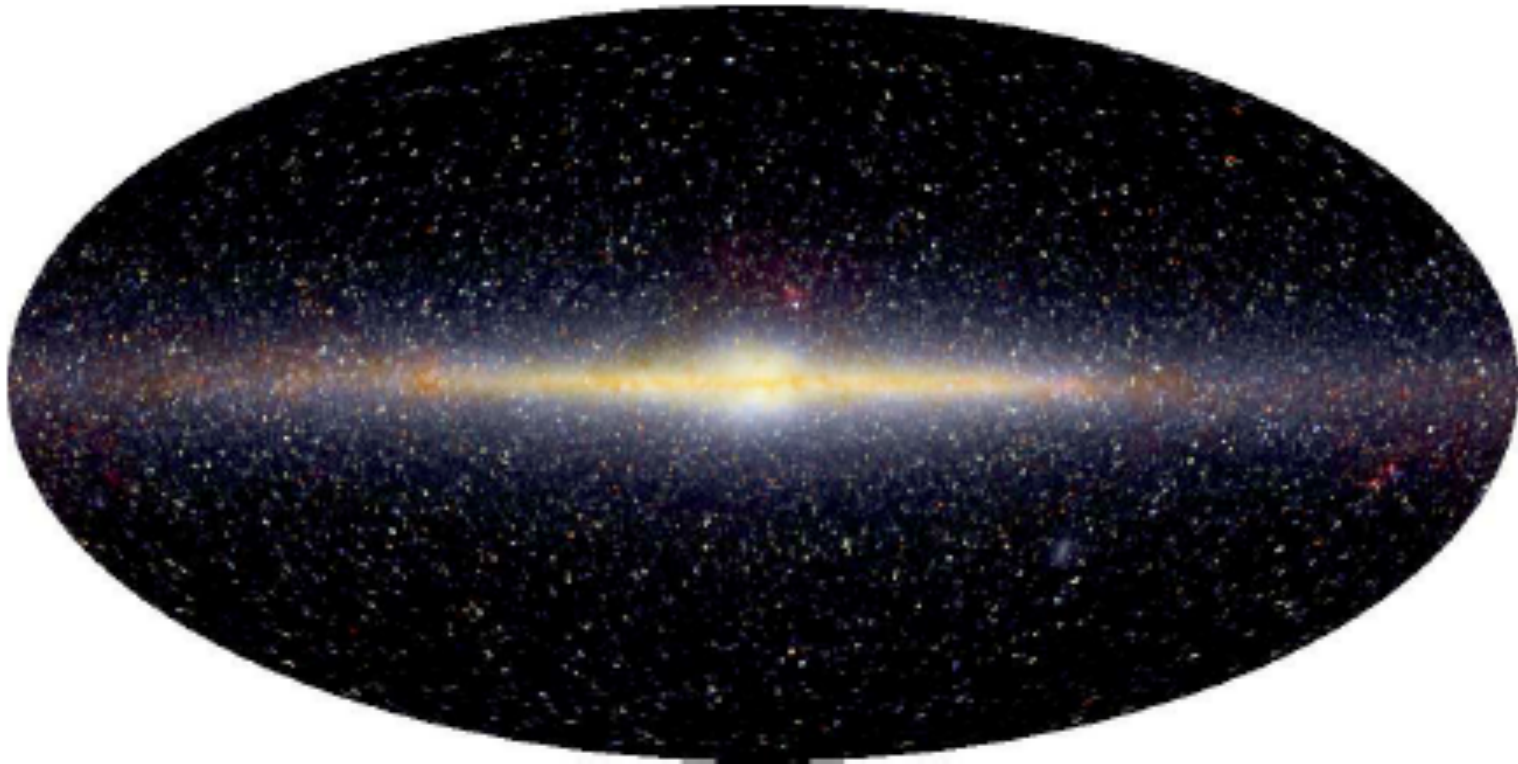


Figure 10 Extinction and scattering calculated for Weingartner & Draine (2001a) model for  $R_V = 3.1$  Milky Way dust, but with abundances reduced by factor 0.93 (see text). The dashed lines show the asymptotic behavior of the absorption ( $\propto \lambda^{-2}$ ) and scattering ( $\propto \lambda^{-4}$ ) cross sections.

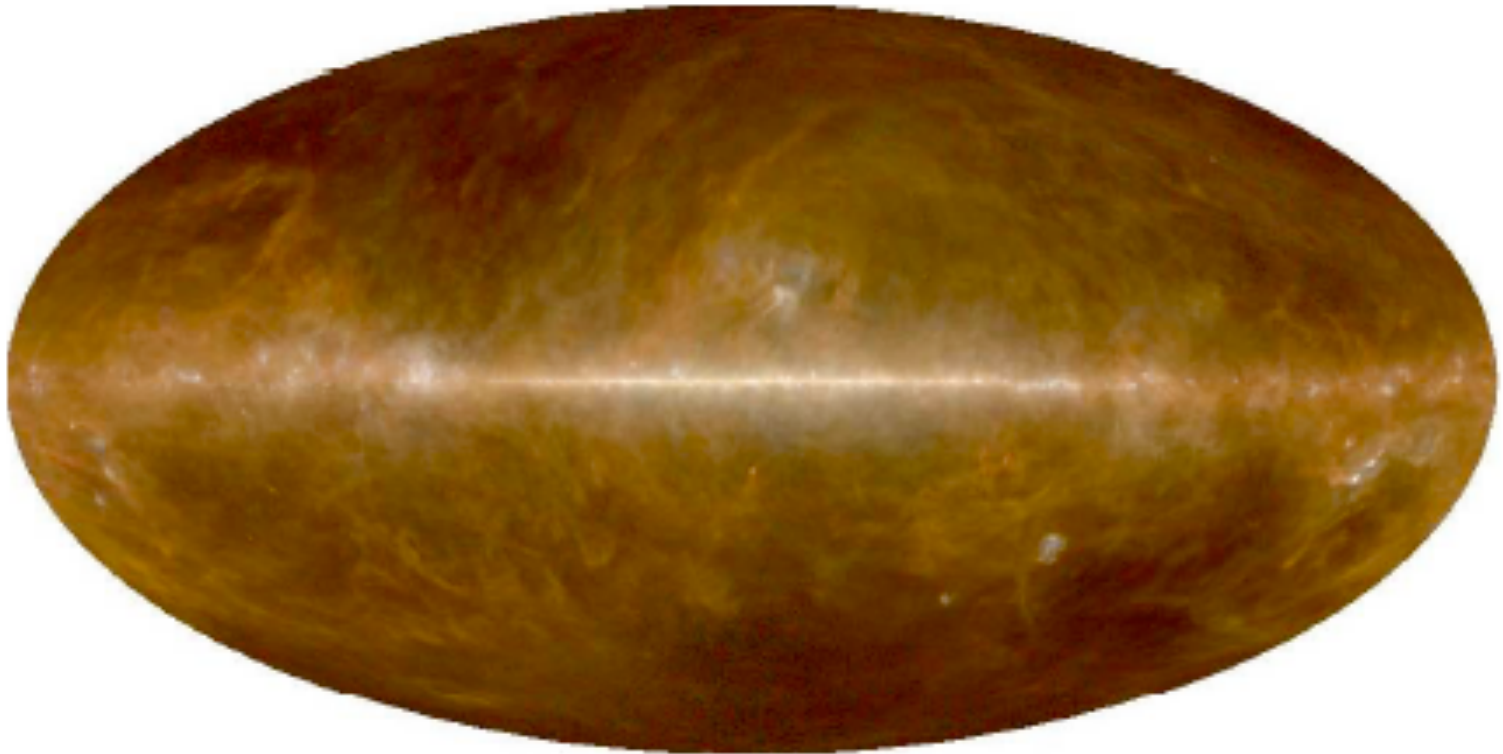
### 3. Dust Thermal Properties

## The Galaxy in the Near-IR



- The sky in the near-IR
  - COBE maps the sky between 1.3  $\mu\text{m}$  and 4 mm
  - The near-IR (*J*, *K* & *L*) shows mostly stars & reduced ISM absorption
  - The disk-like nature of our Galaxy with its bulge is evident

# The Galaxy in the Far-Infrared



- COBE 100, 140 & 240  $\mu\text{m}$ 
  - No ordinary stars, only a few with circumstellar dust shells are weakly detected
  - The bulk of the emission comes from clouds of cool dust ( $\leq 20\text{K}$ )



# **Grain Heating and Cooling**

## **Possible Heating Processes**

- Absorption of starlight
- Collisions with warm gas atoms & molecules
- Chemical reactions on grain surface
- Interaction with cosmic rays

## **Possible Cooling Processes**

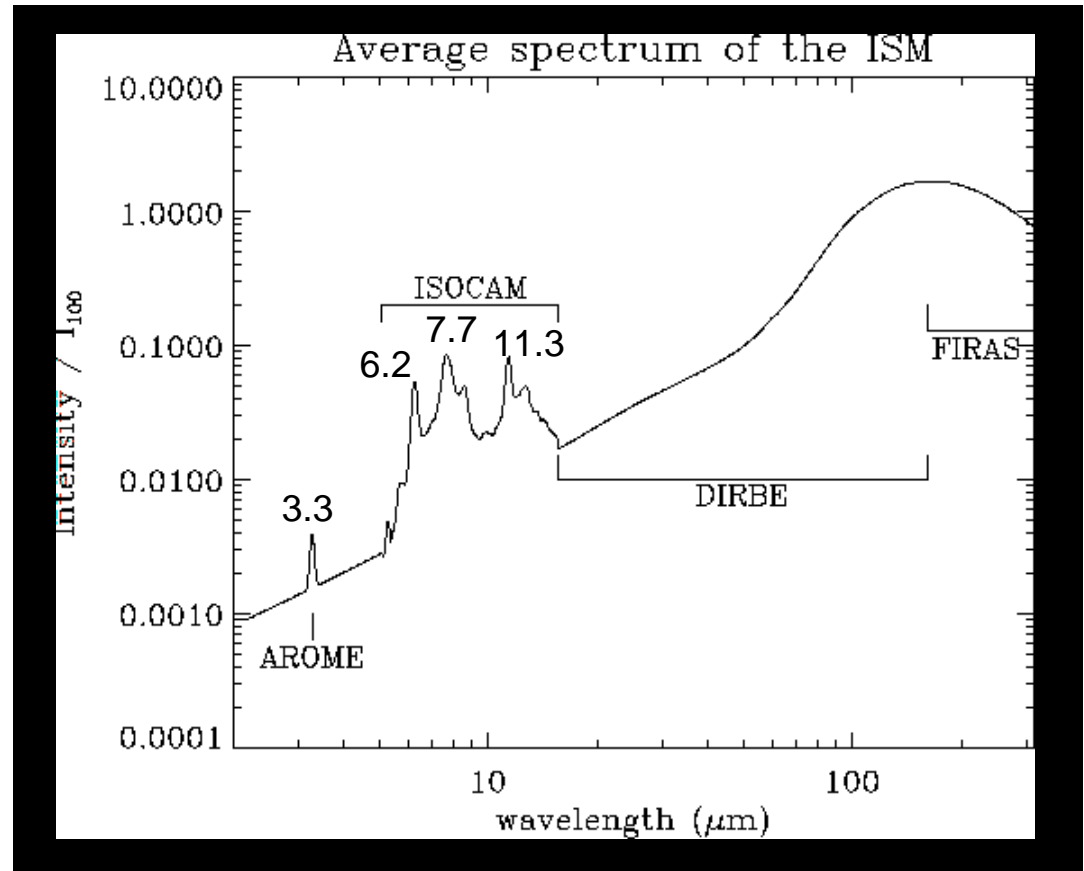
- Radiative cooling (emission of photons)
- Collisions with cool gas
- Sublimation of atoms & molecules from grain surface

**Under most circumstances radiative heating and cooling dominate.**

# Spectrum of the $\rho$ OMC-1 Galaxy in the Far-Infrared

- Bulk of emission c.f.  $\approx 18$  K dust ( $140\text{-}\mu\text{m}$  peak in FIR; see slide in Lec 1)
- Significant  $3\text{-}25\text{ }\mu\text{m}$  emission c.f. warmer grains
- Distinctive features at  $3.3$ ,  $6.2$ ,  $7.7$ ,  $8.6$  &  $11.3\text{ }\mu\text{m}$

**The spectrum of the galaxy shows clear evidence of heating of dust by stars and radiative cooling at infrared wavelengths, i.e., re-radiation of the absorbed starlight at much longer wavelengths by cool grains**



**Mean spectrum of Milky Way IS Dust**  
(Synthesis of balloon & satellite data)

## The Grain Radiative Heating Process

- On absorption of a photon, a grain is left in an excited state. The probability for spontaneous emission is high,  $A \sim 10^7 \text{ s}^{-1}$ .
- Complex grains (as well as molecules with very many energy levels) rapidly convert part of this electronic excitation into vibrational energy on a very short time scale,  $\Delta t \approx 10^{-12} \text{ s}$ 
  - This energy is quickly distributed over the internal degrees of freedom since
$$A \cdot \Delta t \approx 10^{-5} \ll 1,$$
and the grain is heated.

# Heating of Large Grains

- Heating by IS radiation for an *isotropic* radiation field with flux  $F_\lambda = \pi J_\lambda$

$$F_\lambda = \int_{\text{surface}} d\Omega \cos \vartheta I_\lambda = 2\pi I_\lambda \int_0^1 d(\cos \vartheta) \cos \vartheta = \pi I_\lambda = \pi J_\lambda$$

- The heating rate for one grain of radius  $a$  is

$$4\pi a^2 \int_0^\infty \pi J_\lambda Q_a(\lambda) d\lambda = 4\pi a^2 J_{UV}$$

where  $J_{UV}$  is *defined* as

$$J_{UV} \equiv \int_0^\infty J_\lambda Q_a(\lambda) d\lambda$$

**$J_{uv}$  is the rate at which a spherical grain of radius  $a$  absorbs energy from the radiation field per unit surface area. It is weakly dependent on  $a$  for large grains. Most of the heating of large grains c.f. *stellar UV photons* for which  $Q_a \sim 1$ , hence the subscript UV.**

# Steady Thermal Balance

Kirchoff's Law, based on the equilibrium thermodynamics of matter and radiation, relates the emissivity to the absorption coefficient with the Planck intensity function

$$j_\nu(T) = B_\nu(T) \kappa_\nu(T).$$

The power radiated by a grain is then,

$$4\pi a^2 \int_0^\infty \pi B_\lambda Q_a(\lambda) d\lambda$$

and the balance between absorption and radiation is

$$4\pi a^2 J_{UV} = 4\pi a^2 \int_0^\infty \pi B_\lambda Q_a(\lambda) d\lambda$$

$$J_{UV} = \int_0^\infty B_\lambda Q_a(\lambda) d\lambda = \langle Q_a(T) \rangle \frac{\sigma T^4}{\pi}$$

where  $\langle Q_a \rangle$  is the “*Planck average emissivity*”

$$\langle Q_a(a, T) \rangle = \frac{\int_0^\infty B_\lambda Q_a(a, \lambda) d\lambda}{\int_0^\infty B_\lambda d\lambda}$$

# Planck Average Emissivity

$$J_{UV} = \langle Q_a(T) \rangle \frac{\sigma T^4}{\pi}$$

$$\langle Q_a(a, T) \rangle = \frac{\int_0^\infty B_\lambda Q_a(a, \lambda) d\lambda}{\int_0^\infty B_\lambda d\lambda}$$

In the top equation for thermal balance,  $J_{UV}$  is more or less Independent of grain properties, The Planck mean emissivity does vary with  $T$  at small  $T$ , roughly as  $T^2$ , at least according to the Draine & Lee 1984 model. Thus the equilibrium  $T$  is fairly insensitive to the heating level  $J_{UV}$ .

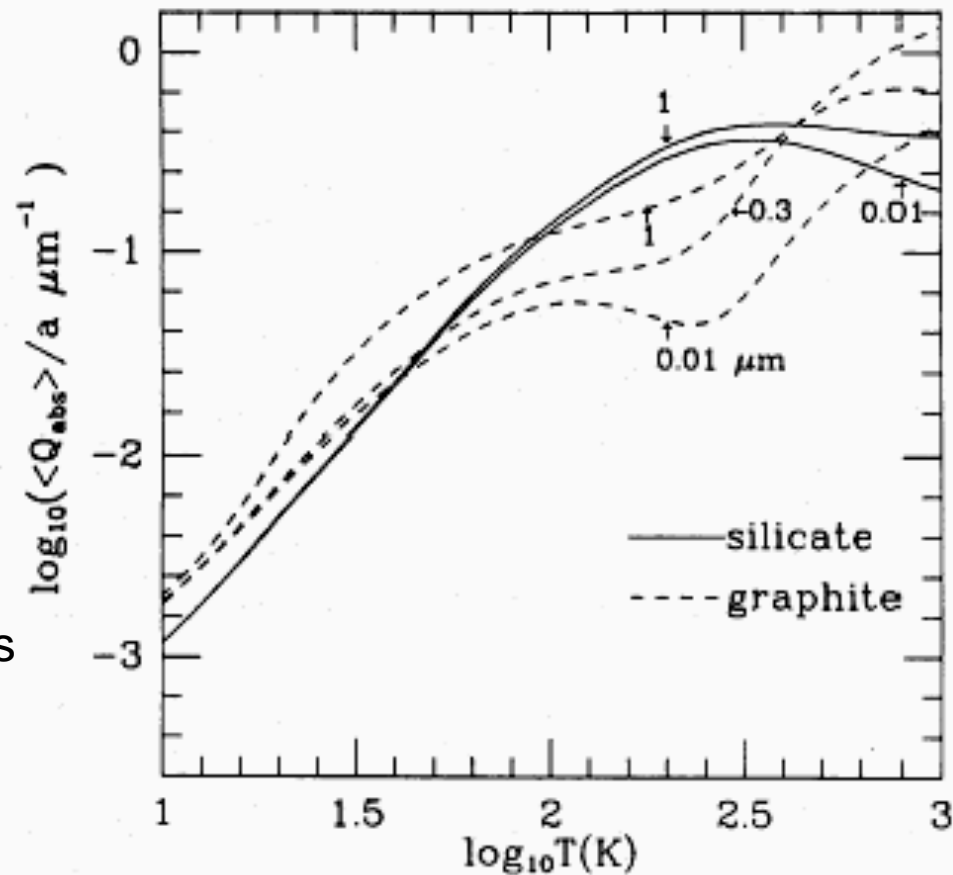


Fig. 11 of Draine & Lee  
ApJ, 285, 89, 1984

# The Temperature of Large IS Grains

**Grains in the diffuse ISM are cold ~ 20 K.**

To calculate  $T_d$ , we need  $Q_a$  in the far-IR. Recall that, according to Mie theory for constant  $m = n - ik$ ,  $Q_a \sim a/\lambda$ , but for realistic dust,  $m = m(\lambda)$ . Typically  $Q_a \sim 1/\lambda^2$  at long wavelengths, as in the Draine & Lee theory. More generally we parameterize the efficiency as  $Q_a \sim a/\lambda^{1+\beta}$ . Thermal balance then reads,

$$J_{UV} \propto \int_0^\infty \frac{2h\nu}{\lambda^2} \left( \frac{1}{e^{h\nu/kT_d} - 1} \right) \frac{a}{\lambda^{1+\beta}} d\nu \propto ah \left( \frac{kT_d}{h} \right)^{5+\beta} \int_0^\infty \frac{x^{4+\beta}}{e^x - 1} dx$$

The equilibrium temperature of a large dust grain

$$T_d \propto (J_{UV}/a)^{1/(5+\beta)}$$

depends weakly on the size of the grain and the strength of the external radiation field.

# Calculated Grain Temperatures

Specify the mean  
radiation field by a  
BB color temperature

$$T_* \approx 5000\text{K}$$

and a dilution factor

$$W \approx 1.5 \times 10^{-13}$$

For  $0.1 \mu\text{m}$  grains,

$$T_d \sim 20 \text{ K.}$$

Small graphite grains are  
hotter because they absorb  
UV more efficiently.

TABLE 3  
TEMPERATURES OF GRAINS IN DIFFUSE  
CLOUDS

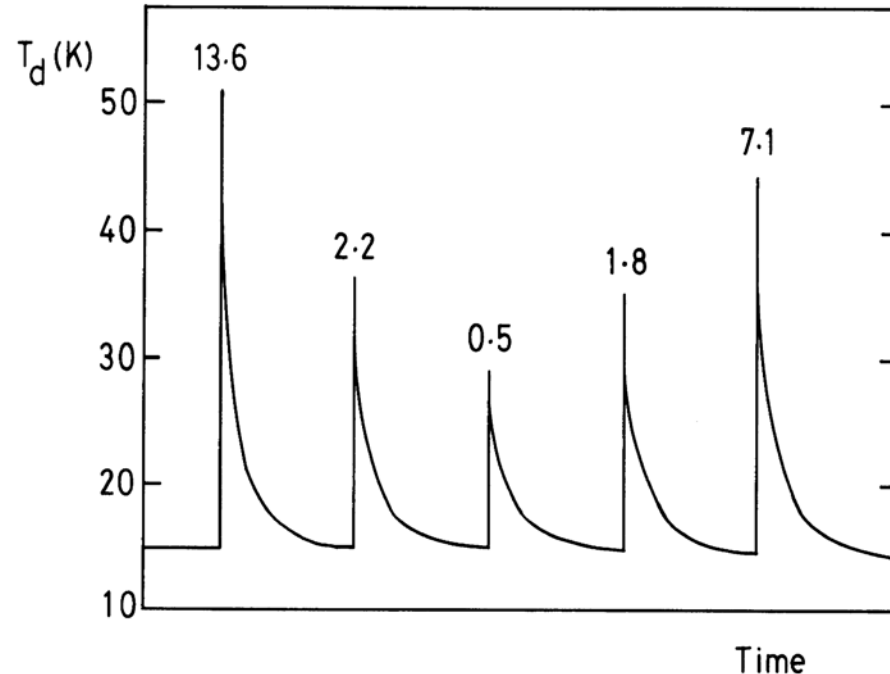
Radius ( $\mu\text{m}$ )	Graphite (K)	Silicate (K)
0.01 .....	20.0	17.9
0.02 .....	19.7	17.3
0.03 .....	19.6	17.0
0.05 .....	19.3	16.5
0.10 .....	18.8	15.4
0.20 .....	17.3	14.9
0.30 .....	16.2	14.7
0.50 .....	14.8	14.4
1.00 .....	12.7	13.4

Draine & Lee , ApJ, 285, 89, 1984



## 4. Small Grains and Large Particles

- Small grains have small heat capacity and small radiating area.
- Absorption of starlight photons leads to temperature spikes.
- A 10 nm grain at 20 K has 1.7 eV of internal energy. Since  $C_v \sim m_{gr} T^3$ , the grain compensates for its small size by getting hot before cooling down.

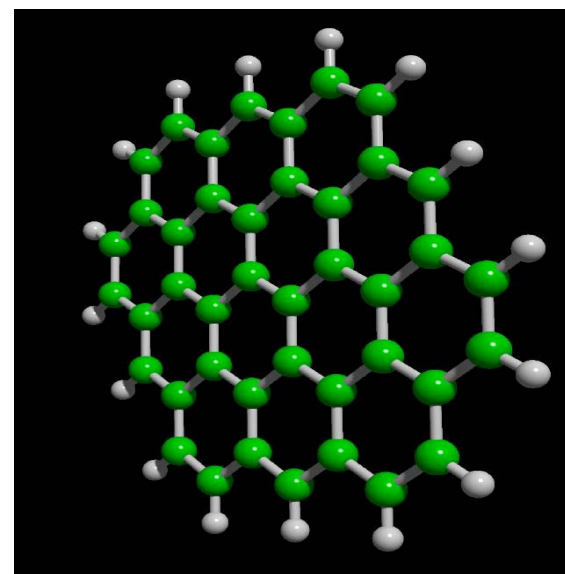


Heating of a small 5-nm grain by individual photons absorbed from the mean IS radiation field. Time between spikes is  $\sim 1$  hr. Cooling by many IR photons, but at shorter wavelengths than expected from equilibrium.

# Tiny Grains and PAHS

Very small grains are more abundant than suggested by the MRN size distribution: The diffuse IR emission of reflection nebulae from 2 - 25  $\mu\text{m}$  is hard to understand unless grains are hotter than expected from the equilibrium considerations of large grains (due to the temperature fluctuations of very small grains).

PAHs



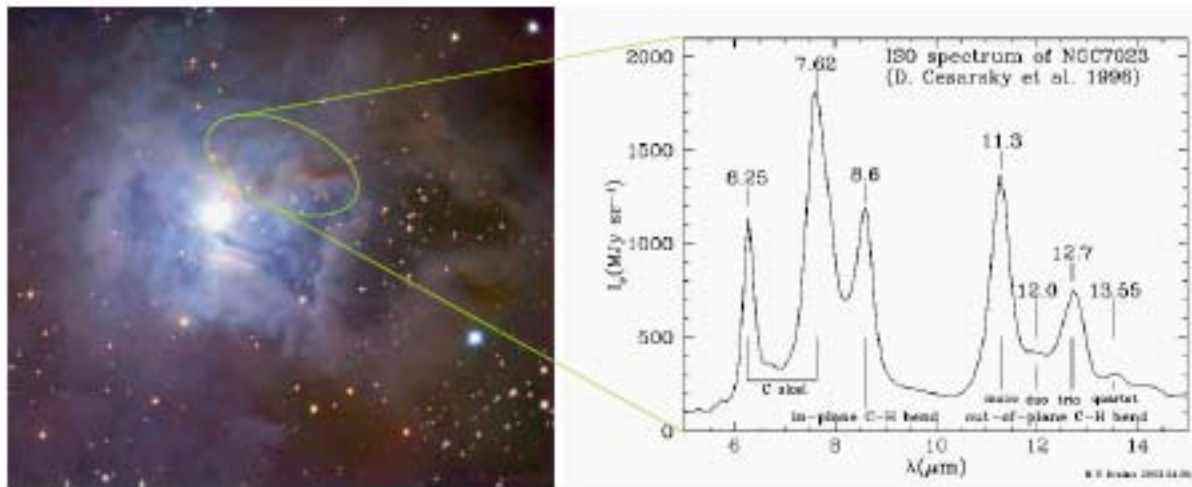
Polycyclic Aromatic Hydrocarbon

PAH molecules are fragments of graphite sheets with edge H atoms; they show characteristic emission at 3.3, 6.2, 7.7, 8.6 & 11.3  $\mu\text{m}$  as observed in warm dust exposed to UV.

# PAHS and Tiny Grains

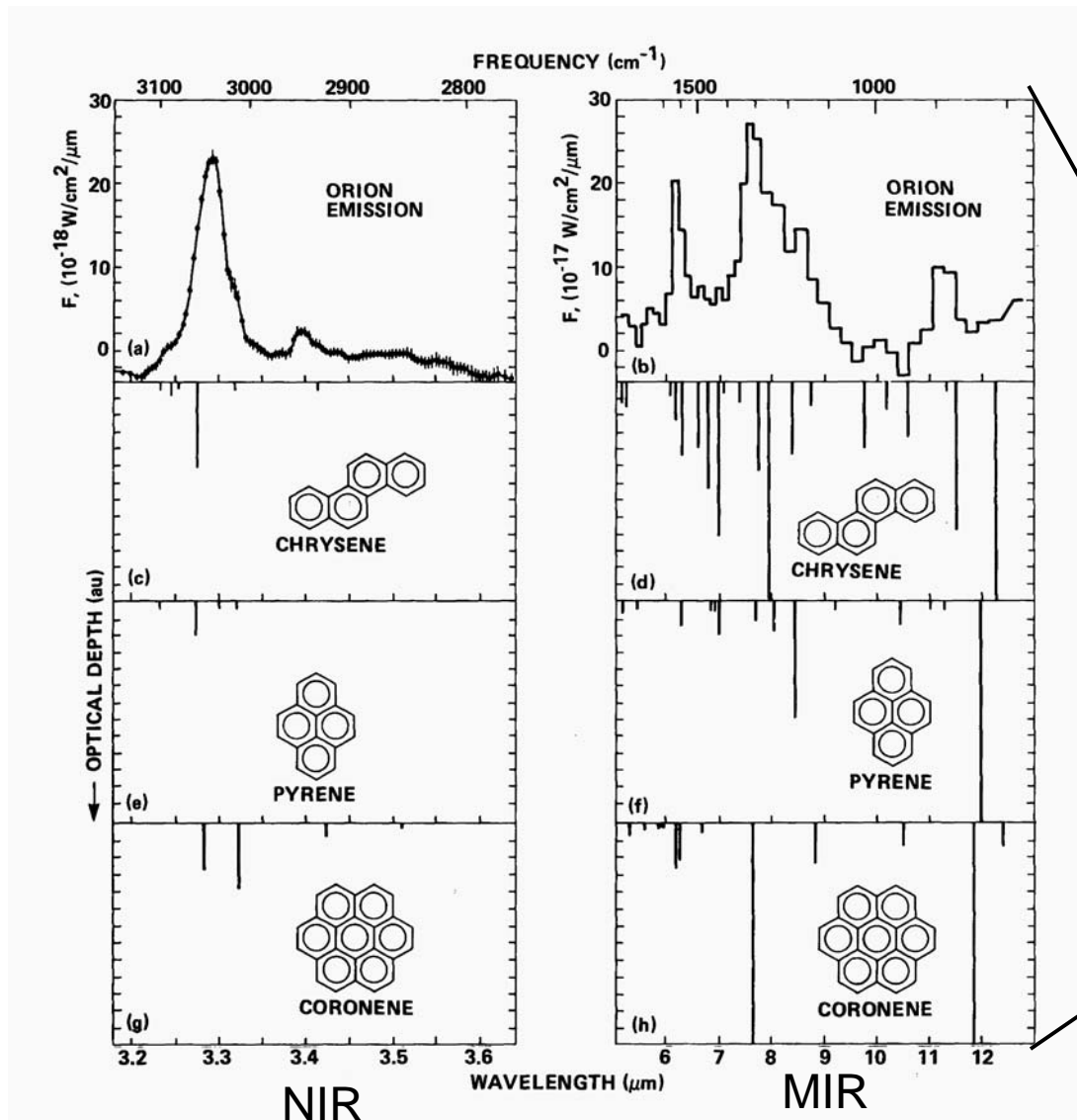
Seen in many warm and irradiated nebulae, such as

- HII regions
- Planetary nebulae
- Reflection nebulae
- Circumstellar around young stars

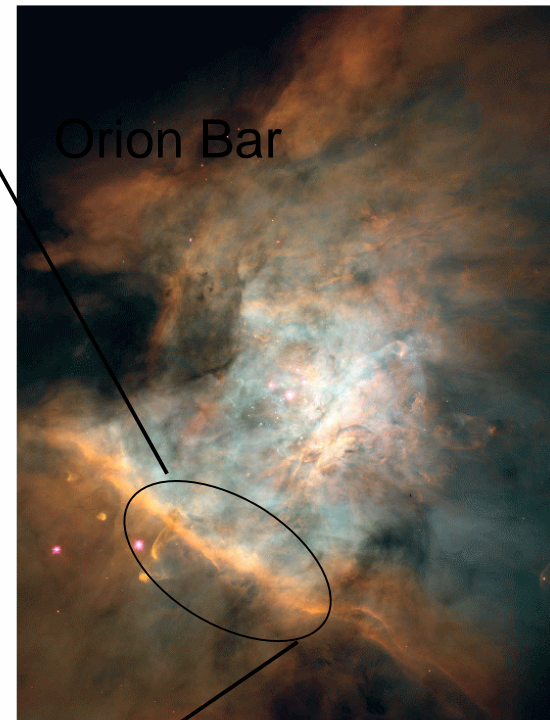


See also the spectrum of the Milky Way (Slide 18) which shows the strong emission from tiny grains and PAHs in the 3-25  $\mu\text{m}$  band

# PAHs & Astronomical Spectra



Orion Bar



**PAHS have many forms, depending on size, hydrogenation, & charge**

# Early Tri-Component Dust Model

## Big silicate grains

$$15\text{nm} < a < 110\text{nm}$$

$$\rho_{\text{dust}}/\rho_{\text{gas}} = 0.0064$$

## Very small graphitic grains

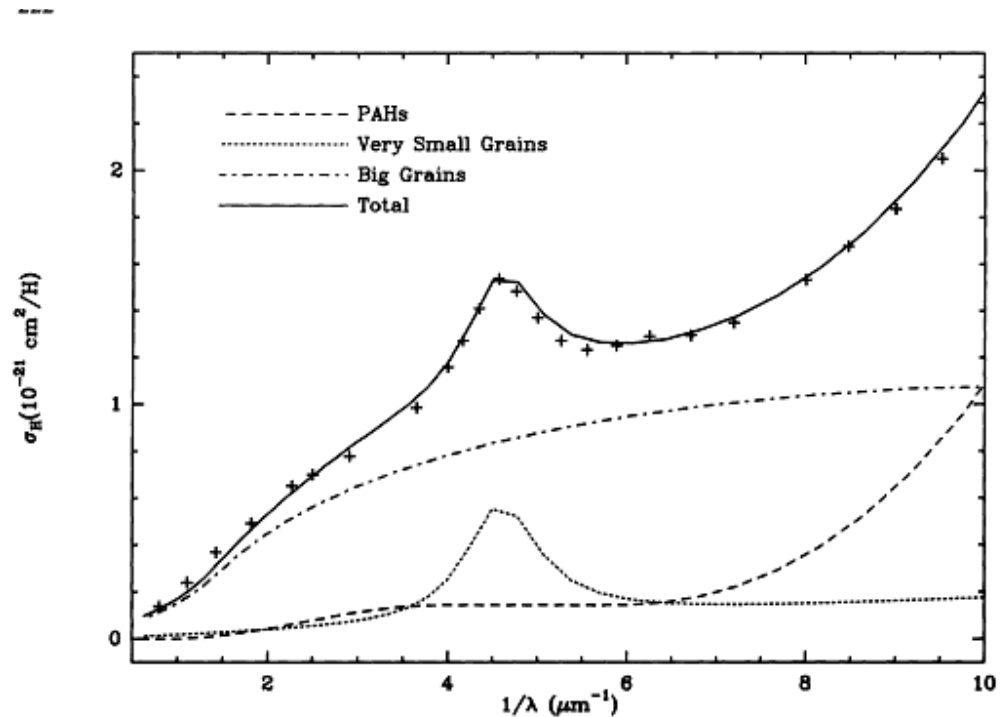
$$1.2\text{nm} < a < 15\text{nm}$$

$$\rho_{\text{dust}}/\rho_{\text{gas}} = 0.00047$$

## PAHs

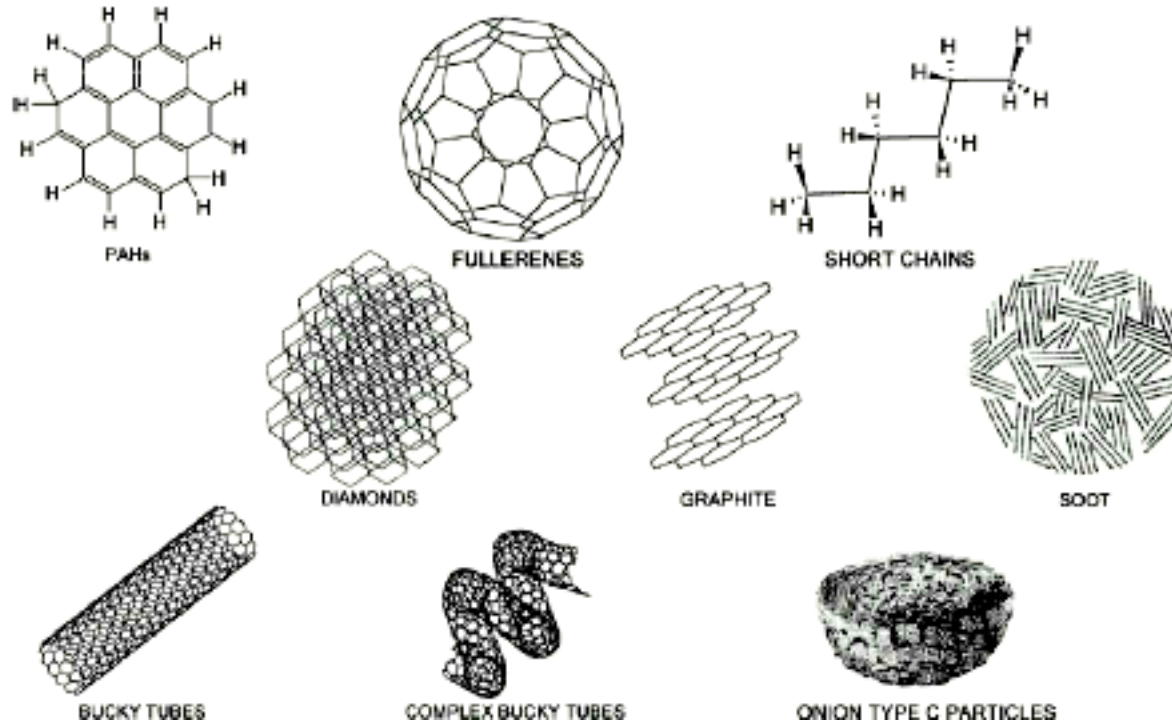
$$0.4\text{nm} < a < 1.2\text{nm}$$

$$\rho_{\text{dust}}/\rho_{\text{gas}} = 0.00043$$



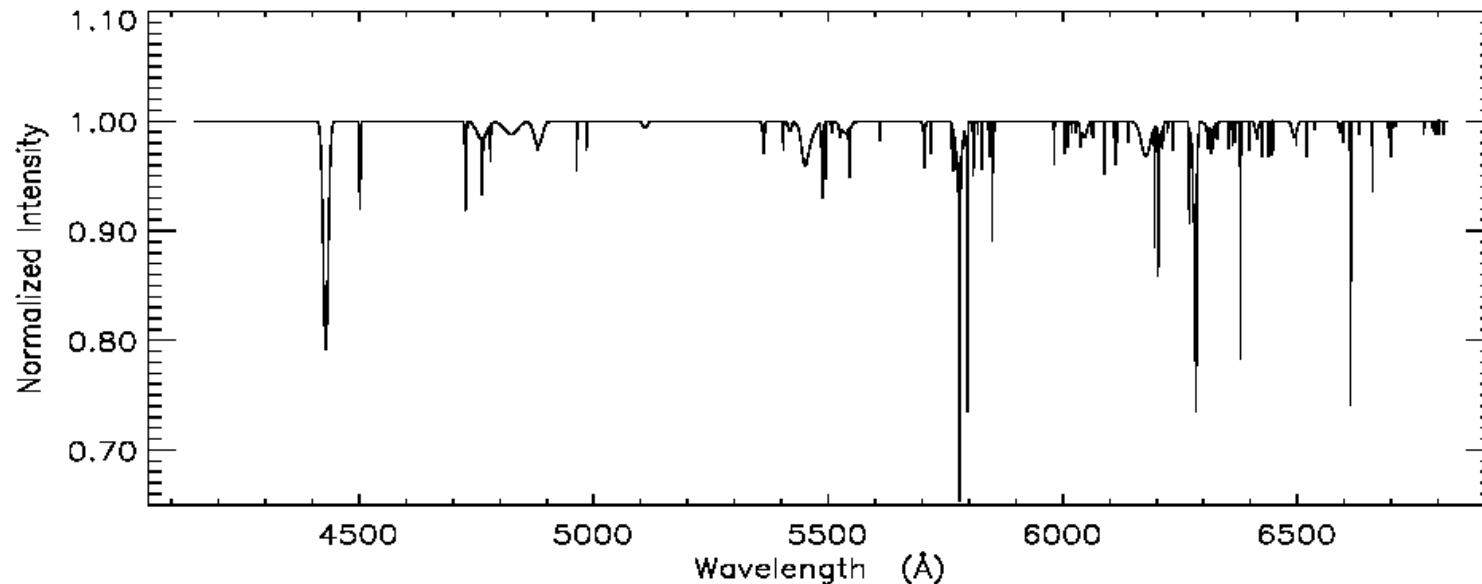
Desert, Boulanger, & Puget  
(AA 237 215 1990). See Draine  
ARAA 41 241 2003 for update.

# Possible Forms of Carbon in the ISM



Some of these have been observed.

# Diffuse Interstellar Bands

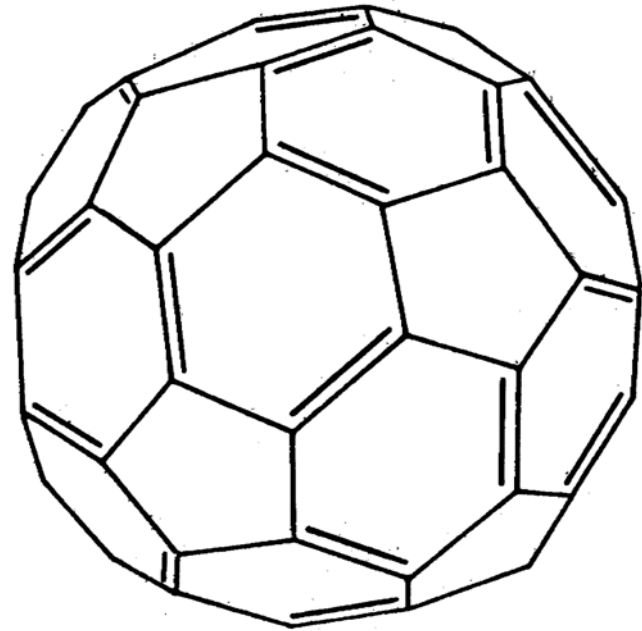


- ~ 200 DIBs known
- Long standing mystery for more than 80 yrs.
- Observed mainly at optical wavelengths in diffuse clouds
- Correlated with atomic rather than molecular hydrogen
- Thought to be electronic transitions of large carbon-bearing molecules such as chains or PAHs

Recent reference: Snow & McCall ARAA, 44, 367, 2006

# Buckminsterfullerene C<sub>60</sub>

- Each C atom connected by one double and two single bonds
- Soccer ball shape
- Closed-shell electronic structure

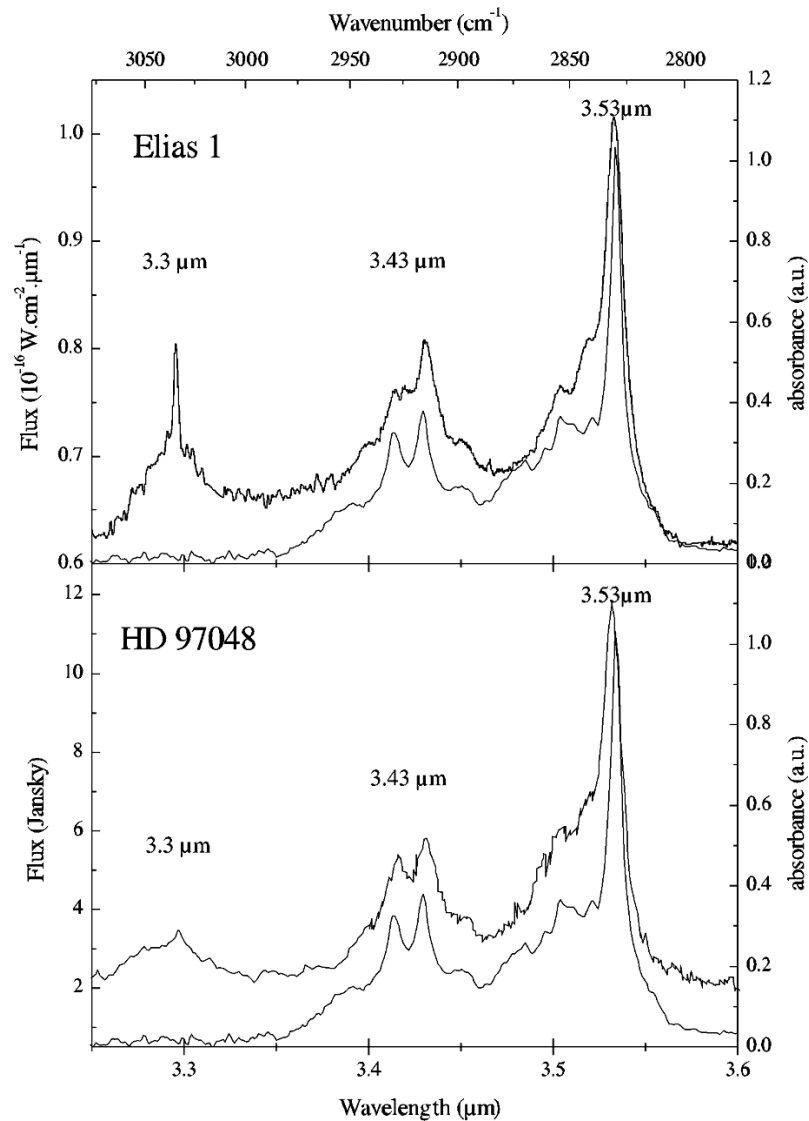


Introduced by Kroto as proposed origin of the polyacetylene chains observed in C-rich AGB stars and in dark clouds. Lab discovery awarded the 1996 Nobel Prize in chemistry.

The identification of C<sub>60</sub><sup>+</sup> with the 9500Å DIBs has been shown to be wrong.



# Circumstellar Diamonds



ISO spectra of two pre main-sequence stars resemble lab spectra of nano-diamond crystals.

## 5. Grain Evolution

Dust grains can change character by interacting with one another and with the gas, especially in dense regions. Examples are:

- *Coagulation* leading to grain growth and changes in the size distribution, manifested by variation of  $R_V$  along different lines of sight & especially its increase in dense regions.
- Cold grains acquire *mantles* of molecular ices, e.g., mixes of  $\text{H}_2\text{O}$ ,  $\text{CO}$ ,  $\text{CO}_2$ ,  $\text{CH}_3\text{OH}$ , etc. They produce characteristic absorption bands towards embedded IR sources.

# Grain Evolution in Translucent Clouds

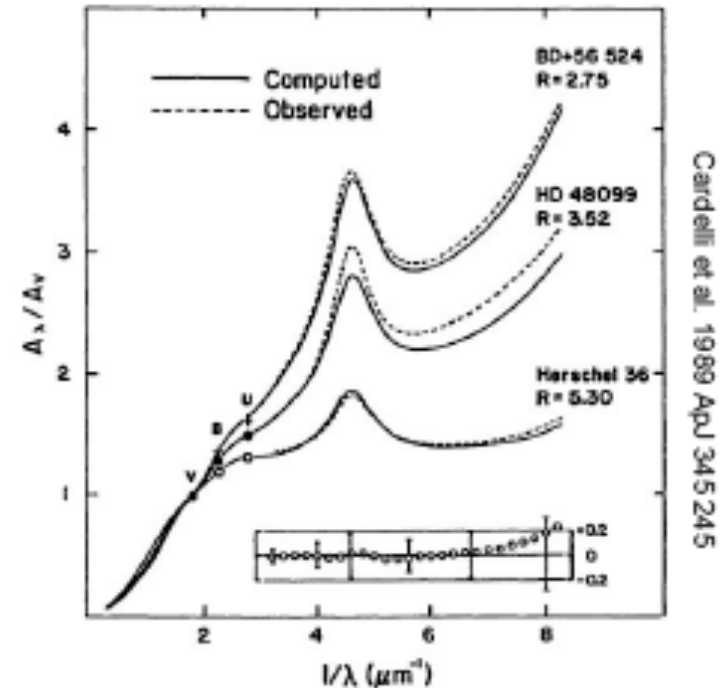
Fits to observed extinction curves by Cardelli et al. (1989) using different values of the normalized extinction

$$R_V = A(V)/E(B-V)$$

with

$$A(V) \sim \lambda^{-\beta}$$

$\beta$	R
0	$\infty$
1	4
1.5	2.5
2	1.8



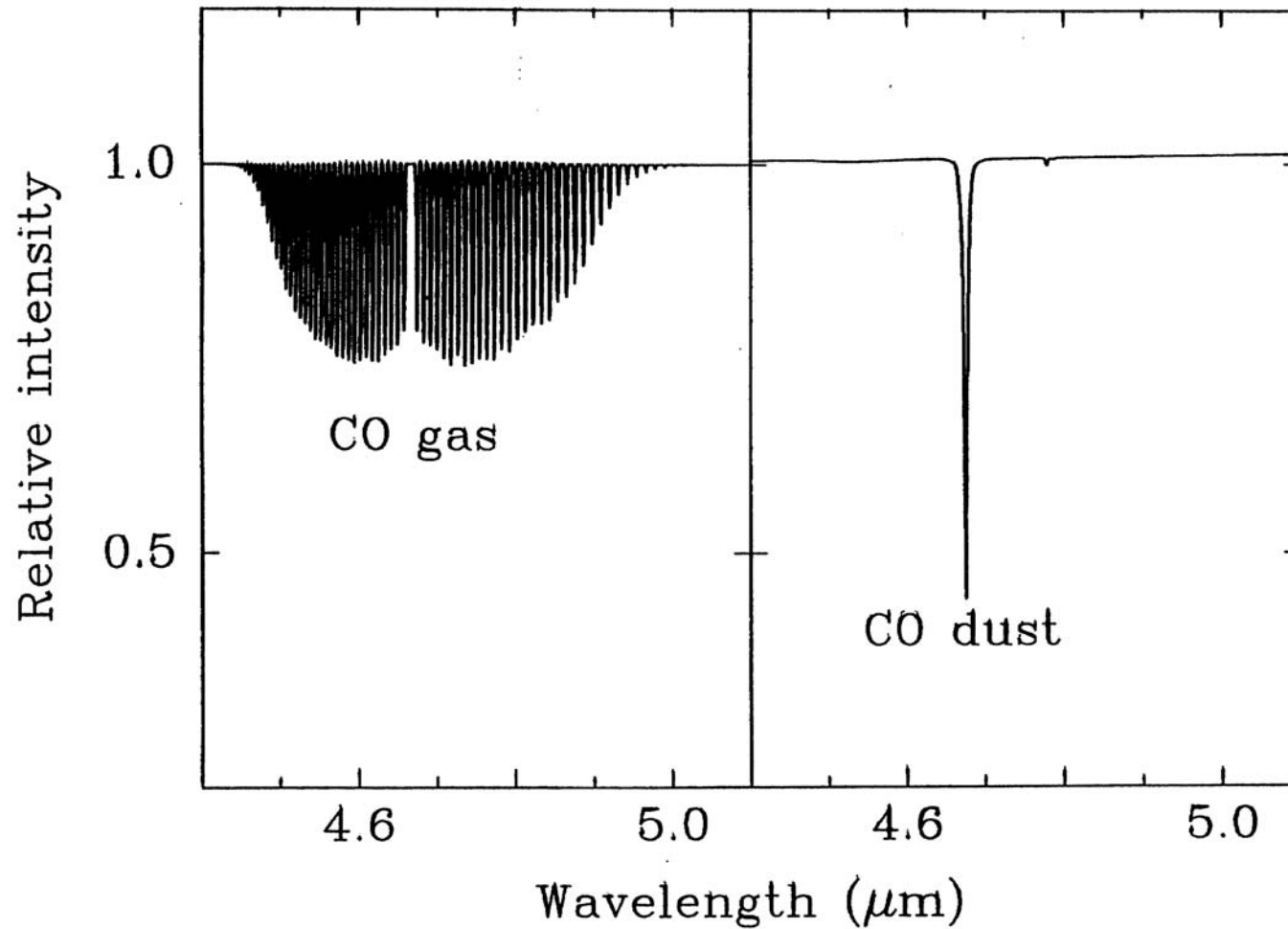
Three *translucent* clouds ( $N_H > 2 \times 10^{21} \text{ cm}^{-2}$ ) whose extinction curves show varying amounts of grain growth

# Spectroscopic Differences Between the Solid and the Gas Phase

- Suppression of rotational structure
  - Molecules cannot rotate freely in ice
    - P, Q, R branches collapse into one broad vibrational band
- Line shifting
  - Interaction of molecules with surroundings modifies force constants
- Line broadening
  - Interaction with ice environment: molecules are located at slightly different sites
    - Bands are broadened
    - Broadening depends on species

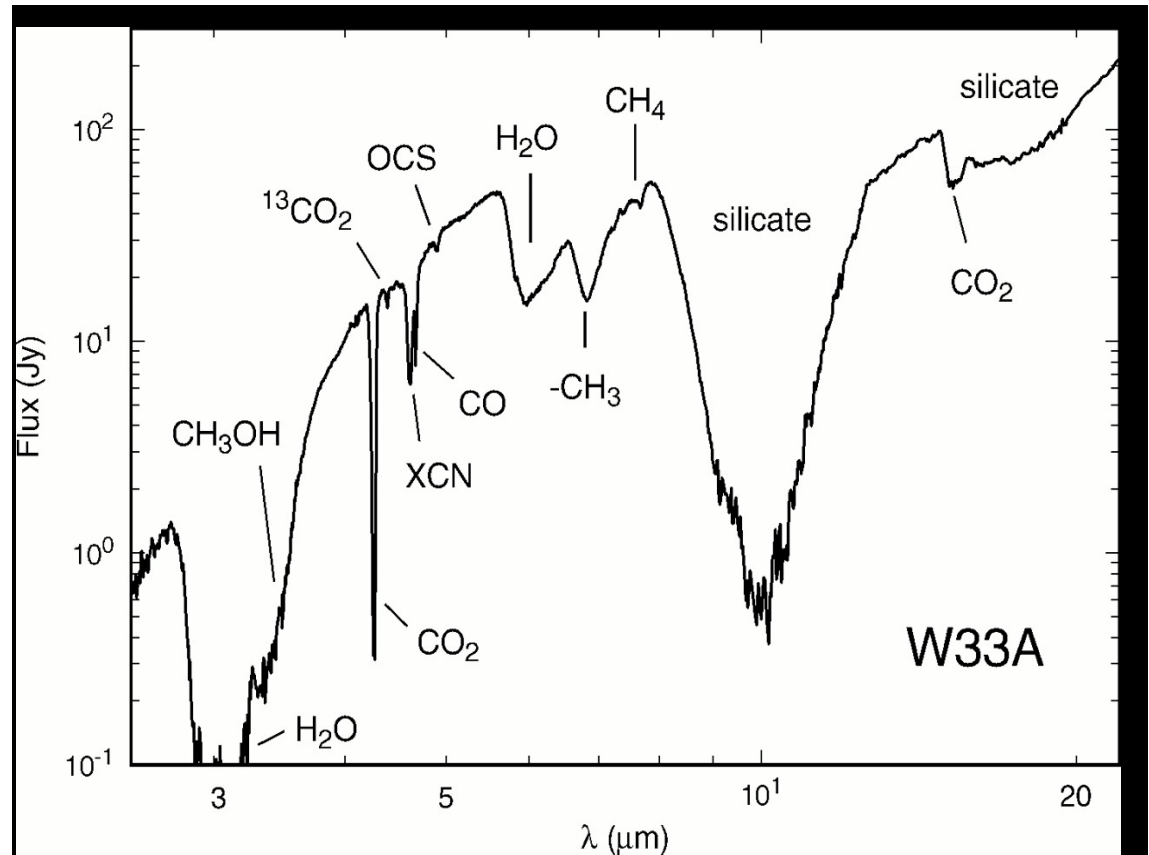
# Gas-Phase and Solid CO

Fundamental ro-vibrational  $v = 1-0$  bands



# Observation of Interstellar Ices

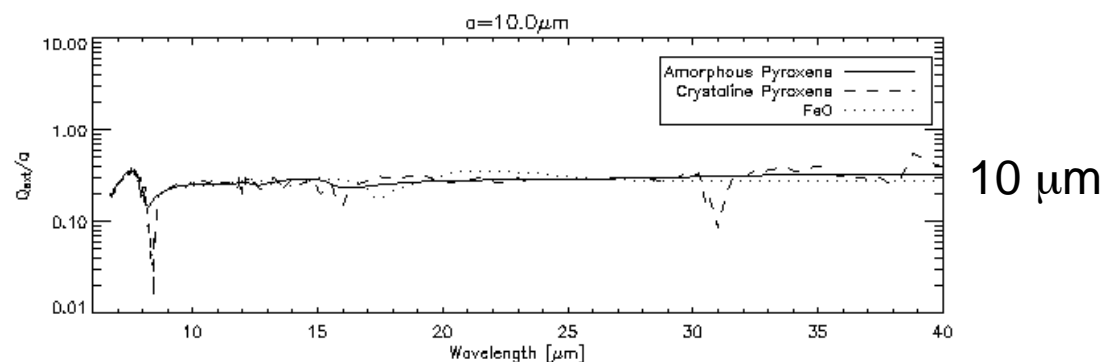
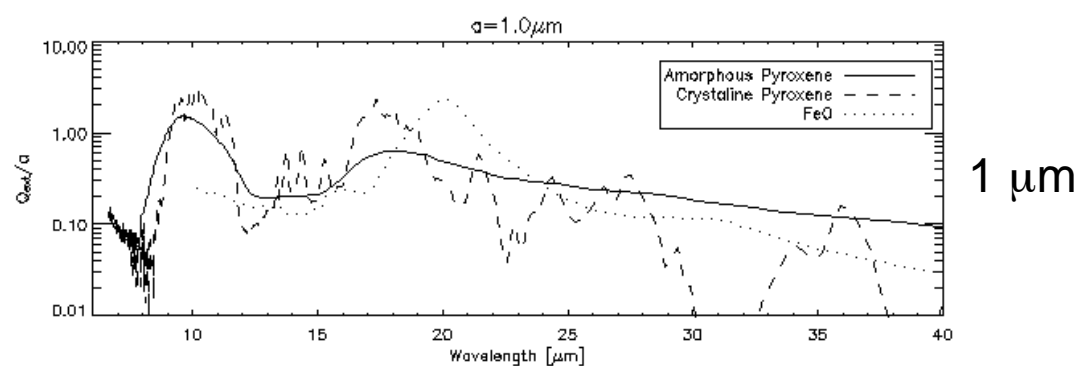
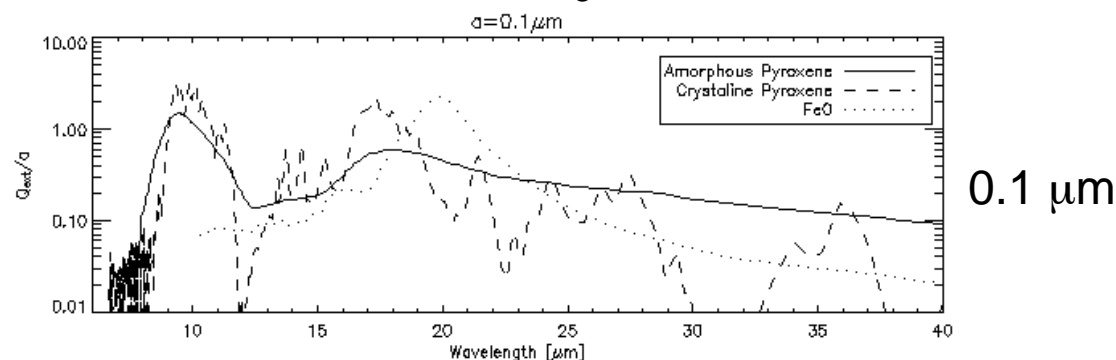
- 3.1  $\mu\text{m}$ : amorphous, dirty  $\text{H}_2\text{O}$  ice
- 4.27  $\mu\text{m}$ :  $\text{CO}_2$  stretching
- 4.6  $\mu\text{m}$ : CN stretch (XCN,  $\text{OCN}^-$  ?)
- 4.67  $\mu\text{m}$ : CO
- 6.0  $\mu\text{m}$ :  $\text{H}_2\text{O}$  bending
- 6.8  $\mu\text{m}$ : ?
- 15  $\mu\text{m}$ :  $\text{CO}_2$  bending



**Solid-state absorption bands in clouds towards an embedded IR source.**

# Amorphous & Crystalline Solids

Mid-IR Spectra vs. Grain Size  
Pyroxenes (Mg, Fe, Ca)SiO<sub>3</sub> vs. Grain Size



The silicate feature disappears for large grains